Wear 414–415 (2018) 327–340

Contents lists available at ScienceDirect

Wear

journal homepage: www.elsevier.com/locate/wear

Influence of surface modification on wear behavior of fly ash cenosphere/epoxy syntactic foam

Kiran Shahapurkar, Vikas Bapurao Chavan, Mrityunjay Doddamani*, G.C. Mohan Kumar

Lightweight Materials Laboratory, Department of Mechanical Engineering, National Institute of Technology Karnataka, Surathkal 575025, India

ARTICLE INFO

Keywords:
Surface modification
Syntactic foams
Cenospheres
Wear

ABSTRACT

The present study deals with investigating the surface modification effect of fly ash cenosphere (as received and surface treated) on the friction and wear response of epoxy syntactic foams. Such lightweight syntactic foams have the potential in using them as tribo-materials for friction applications like in brake pad composites. This study also addresses the environmental linked disposal issues of fly ash cenospheres by incorporating them (up to 60 vol%) in the epoxy matrix. Cenosphere content and surface modification influence on the friction and wear response of cenosphere/epoxy syntactic foams is investigated against EN31 steel disc under dry sliding conditions. Wear behavior is studied at room temperature for different velocities (2 and 5 m/s), applied loads (30 and 50 N) and sliding distances (3, 5 and 7 km). Neat epoxy exhibits maximum wear rate as compared to foams. Wear rate decreases with increasing sliding distance and cenosphere content at all tested conditions. With the increase in the applied load and the sliding velocity, higher wear rate is noted for neat epoxy samples while it decreases with increasing filler loading. Surface modified cenosphere reinforced foams exhibit better wear resistance compared to as received cenosphere dispersed foams and neat epoxy for all the operating conditions owing to the good interfacial bonding of treated cenospheres with epoxy matrix. Specific wear rate decreases significantly with an increase in applied load. Further, the coefficient of friction decreases with higher filler loading and surface modifications. Scanning electron microscopy is used to study the wear mechanisms. Wear debris is analyzed and disc temperature is also reported. Finally, wear rate results are summarised and compared with the data available from literature and are presented in a property map.

1. Introduction

Weight sensitive structures demand higher specific properties necessitating the usage of lightweight polymer matrix composites like syntactic foams. Syntactic foams are realized by infusing hollow microballoons in the matrix resin and find applications in naval, transportation and aerospace components because of better damage tolerance coupled with lower weight [1,2]. Other applications of these closed cell foams include buoys, underwater vehicle components, buoyancy modules and sports goods [3,4]. Syntactic foams have also been explored for automotive brake lining applications as friction materials [5]. Although polymer syntactic foams are being widely investigated for developing lightweight components/structures in weight sensitive regime, friction and wear behavior investigations are seldom reported when compared with solid particulate filled composites targeted as tribo-materials for friction applications, like in brake pads. As wear is the most common phenomena in such applications, there is an increasing thrust in developing materials with higher specific properties keeping lower constituent costs and processing therein [6,7]. Wear mechanisms are influenced by constituent materials, geometry, processing conditions, surface modification, filler content etc., necessitating an understanding of their influence on structure-property correlations. Lower cost of the fillers is governed by high volume availability. One such inexpensive, environmentally pollutant filler is fly ash. Thermal power plants are the source of fly ash and are a waste by-product needing effective disposal [8–10]. Cenosphere (hollow microballoon) is the major constituent in fly ash [11,12]. SiO_2, Al_2O_3 and Fe_2O_3 forms nearly 90% of the total cenosphere composition. Other compounds such as K_2O, MgO, CaO, TiO_2, and Na_2O are present in negligible quantities. Cenospheres comprise ceramic elements like silica and alumina as the primary constituent elements [13]. Low density fly ash cenospheres are very beneficial to attain higher strength to weight ratio [14,15]. Addition of aluminum oxide, silicon carbide (constituent element of cenosphere), copper oxide, titanium dioxide, zinc oxide and zirconium dioxide in polymers significantly improve the wear resistance [16–20]. Fly ash cenospheres are spherical in shape, readily

* Corresponding author.
E-mail address: mrdoddamani@nitk.edu.in (M. Doddamani).

https://doi.org/10.1016/j.wear.2018.09.001
Received 19 April 2018; Received in revised form 2 September 2018; Accepted 5 September 2018
Available online 10 September 2018
0043-1648/

Nomenclature

ρ	Density of the composite (kg/m^3)	D	Sliding distance (mm)
ρ^{th}	Theoretical density (kg/m^3)	w_t	Wear rate (mm^3/km)
ρ^{exp}	Experimental density (kg/m^3)	w_r	Wear resistance (km/mm^3)
ϕ_V	Void content (%)	w_s	Specific wear rate (mm^3/km-N)
V	Sliding velocity (m/s)	F	Applied force (N)
W	Wear volume	μ	Coefficient of friction
		F_T	Tangential force (N)
		F_N	Normal force (N)

available in particulate form, inexpensive and possess superior mechanical properties [21–25]. Landfill burden and disposal related issues pertaining to fly ash cenospheres can be effectively addressed if these hollow particles are incorporated in most commonly used thermosetting matrix like in epoxy resin. Such an effort is successfully demonstrated, as presented herewith, which might lead to the development of utilitarian syntactic foams for tribological applications [8,26,27]. Further, while improving the mechanical and thermal characteristics, syntactic foams become economical due to the incorporation of low-cost cenospheres [28–31].

Composites containing hollow particles can have significant differences in their tribological behavior and wear mechanisms as compared to those reinforced with solid particles. Void space enclosed inside the hollow particles open up due to partial wear resulting from shearing off of the thin porous shell. These void spaces can accumulate wear debris and provide a smoother surface that enhances wear resistance [32]. Detailed investigation for understanding the mechanisms of wear and damage in naturally available hollow microballoons with variable wall thickness and in-situ wall thickness porosity is the need of the time and is highly desired. Al/cenosphere syntactic foams wear response is observed to be influenced significantly by craters formed as microballoon fractures [14]. Tribological behavior of cenosphere reinforced polymeric composites is dealt elaborately in the available literature [33–36]. Effect of cenosphere particle size on tribological behavior of polyester composites is reported in Ref. [33]. Composites with cenospheres of 300 nm size show higher wear resistance. Effect of material, geometry and process parameters on tribological behavior of vinyl ester foams is studied by Chauhan et al. [34]. Findings suggest that the wear resistance of syntactic foams improved with submicron and micro-sized cenospheres. Investigation of the abrasive behavior of silane modified cenospheres on LDPE foams by Chand et al. [35] revealed 10 wt% of cenospheres show optimum tribological properties. Cenosphere particles of submicron size enhance the wear resistance in comparison to micron-sized fillers [34]. Fly ash cenospheres in as received condition are used with vinyl ester, polyester and epoxy matrix for studying the tribological properties. Surface modification of cenospheres promotes interfacial bonding which might result in enhanced wear resistance. From the existing literature, it is observed that the tribological response of surface treated naturally available hollow fillers reinforced in the thermosetting matrix is yet to be reported [33,34]. Cenosphere-reinforced thermosetting matrix composites are investigated elaborately for structural applications [32,37–39]. Increasing demand on the usage of closed cell foams in transportation and aviation sectors necessitates a better understanding of their friction and wear characteristics. Fly ash cenospheres being naturally available, have surface defects on the exterior surface and within the shell wall thickness. Interfacial bonding between the constituents determines the improvement in overall mechanical properties [40,41]. Surface modification of cenospheres is a viable option in achieving superior interfacial topology and tribological behavior [39]. Suitable coupling agent enhances interfacial bonding between the constituent materials through a molecular bridging phenomena. Silane is the most widely used coupling agent for surface modification of fly ash cenospheres for making them compatible with most of the resins [40,41].

Present work aims to gain an understanding on the role of surface treatment of cenosphere filler on the wear mechanism of hollow particle filled composites and to identify critical parameters that aid in the development of better friction material, in the context of weight saving potential and tribological performance. In this regard, the wear test as presented herewith are not designed to reproduce real braking conditions for which specific equipment, like dynamometer rigs and bench test apparatuses, are available, and is the focus of our future studies. Though the pin-on-disc (PoD) apparatus doesn't simulate all aspects for the intended application, PoD apparatus has extensively been used to investigate the friction and wear behavior of materials designed to be used in vehicular brake systems in various transportation fields such as trains and road vehicles under steady conditions [42,43]. Further, these PoD tests aid in obtaining useful information on the structure-property relationships of automotive friction materials and serve as verification tests to model the wear and lubricant behavior of materials having a linear relative velocity such as in brake pads [44].

Many structural members experience higher magnitudes of sliding velocity, applied load and sliding distance and are presented in this work. Influence of silane treated cenosphere/epoxy foams is not yet reported with a focus on debris analysis and disc temperature rise. Investigations of surface modified fly ash cenosphere filled thermoset syntactic foams needs to be studied to know the benefits of filler surface modification. Untreated and silane modified cenospheres are dispersed in the epoxy matrix by 20, 40 and 60 vol%. Neat epoxy samples are prepared for comparison. Effects of sliding velocity applied load and sliding distance on the wear rate, specific wear rate and coefficient of friction are investigated. To correlate the observed results, scanning electron microscopy of the worn surface are performed, wear debris are analyzed and the temperature rise of the disc is reported. Finally, property map is presented which might act as a guideline for industrial practitioners while choosing appropriate composition for dry sliding wear response based on the devised applications.

2. Materials and test methods

2.1. Materials

Epoxy resin (Lapox L-12, K-6 hardener) procured from Atul, Valsad, Gujarat is used as the matrix. Table 1 presents chemical and physical results of cenospheres (Cenosphere India Ltd., Kolkata). 3-Amino propyl triethoxysilane (APTS) is supplied by Sigma Aldrich, Bangalore, India and is used for cenosphere surface treatment. Particle size analysis and confirmation of silane coating on the filler is carried out and the details are available in Ref. [24,45].

2.2. Syntactic foam fabrication

Cenospheres by 20, 40 and 60 vol% are dispersed in epoxy gently to obtain a homogeneous slurry. Subsequently, 10 wt% hardener is added into the mixture and finally degassed for 5 min before pouring it in aluminum molds. Room temperature curing of 24 h followed by curing at 90 °C for 3 h is adopted. Similar processing methodology is followed for preparing foams with cenospheres for both untreated and treated surface conditions. For comparative analysis, neat epoxy slabs are also cast. Samples thus prepared are coded as per EXX-Y convention, where

Table 1
Physical chemical and sieve analysis details of cenospheres.[a]

Physical properties		Chemical analysis		Sieve analysis	
True particle density	920 kg/m^3	SiO_2	52–62%	+30 # (500 μm)	Nil
Bulk density	400–450 kg/m^3	Al_2O_3	32–36%	+60 # (250 μm)	Nil
Hardness (MOH)	5–6	CaO	0.1–0.5%	+100 # (150 μm)	Nil
Compressive strength	180–280 kg/m^2	Fe_2O_3	1–3%	+150 # (106 μm)	0–6%
Shape	Spherical	TiO_2	0.8–1.3%	+240 # (63 μm)	70–95%
Packing factor	60–65%	MgO	1–2.5%	+240 #	0–30%
Wall thickness	5–10% of shell dia.	Na_2O	0.2–0.6%		
Color	Light grey	K_2O	1.2–3.2%		
Melting point	1200–1300 °C	CO_2	70%		
pH in water	6–7	N_2	30%		
Moisture	0.5% max.				
Loss on ignition	2% max.				
Sinkers	5% max.				
Oil absorption	16–18 g/100 g				

[a] As specified by supplier.

E, XX, Y represents epoxy resin, filler content by volume % and surface treatment mode (U - untreated, T - treated) respectively. Sample dimensions are followed as per ASTM G99-17 standard [38]. ASTM D792-13 [39] is followed to compute densities of all the samples. Theoretical density (ρ^{th}) is calculated using,

$$\rho^{th} = \rho_f V_f + \rho_m V_m \tag{1}$$

where f denotes filler and matrix is represented by m.

Void content (ϕ_V) is computed using [22,24],

$$\phi_V = \frac{\rho^{th} - \rho^{exp}}{\rho^{th}} \tag{2}$$

2.3. Wear test

Wear test in dry mode is conducted at ambient conditions as outlined in ASTM G99-17 [38] using tribometer (TR-20LF-PHM400-CHM600) procured from DUCOM, Bangalore, India. Rotor discs in automotive braking systems are most commonly made of grey cast iron and steel due to their excellent damping capacity, higher wear resistance, better thermal conductivity and lower costs of production coupled with ease of machining [46–48]. Thus, the EN-31 disc having 62HRC hardness is used for investigating wear response of developed samples. The tests are carried out on 120 mm diameter track with 318 and 795 rpm corresponding to 2 and 5 m/s sliding velocities.

Table 2 lists the parameters and their values used for the experimentation. Sliding velocity applied load and sliding distances are represented as V_a, F_b, and D_c. Subscripts a, b and c represent the respective values of the parameters. Two average nominal contact pressures, P_o, are investigated: 0.21 and 0.35 MPa corresponding to a normal load of 30 N and 50 N, respectively. These conditions are chosen to simulate low and mild sliding wear conditions for brake applications in which the P_oV_a value (given by the product of the contact pressure and the sliding velocity) range between 0.3 and 20 MPam/s [49–51]. The width of the wear track is 12 ± 0.01 mm. The disc is polished with SiC paper (600 grit) prior to each test for maintaining constant surface roughness value of 0.11 μm. The sample with dimensions of 12 × 12 × 25.4 mm is clamped firmly in the sample holder and the test is carried as elaborated in Ref. [38]. Three replicates are tested for each composition to ensure repeatability and the average values are reported. Frictional force and height losses are recorded. Pin cross-sectional area is used to compute the volume loss. Sliding distance is calculated from sliding speed and the time elapsed. Wear rate (w_t) is determined by,

$$w_t = \frac{W_C - W_B}{d_C - d_B} \tag{3}$$

where subscripts C and B corresponds to end and start of steady-state wear. Wear rate varies with applied normal load and is independent of sliding distance. Wear resistance is reciprocal of wear rate and is given by,

$$w_r = w_t^{-1} \tag{4}$$

Specific wear rate (w_s) accounts for the load carrying capacity and is computed using,

$$w_s = \frac{w_t}{F} \tag{5}$$

The coefficient of friction (μ) is defined as,

$$\mu = \frac{F_T}{F_N} \tag{6}$$

2.4. Temperature measurement, EDS and SEM

The temperature of the steel disc after the completion of each test is measured using a thermocouple (CMPH – x, HAMI THERM, Netherlands). Energy Dispersive Spectroscopy (EDS) (JSM 6380LA, JEOL, Japan) is carried out on the wear debris to identify the prominent wear mechanism. Scanning electron microscope (SEM) of JEOL make (JSM 6380LA) is utilized for micrography while JFC-1600 is used for gold coating of samples are for better conductivity. Micrography is performed on the worn surface to analyze the dominant wear mechanism.

3. Results and discussions

3.1. Material processing and micrography

Micrographs of untreated and silane coated cenospheres at the same magnification levels are presented in Fig. 1. Due to a very small layer thickness of silane coating, it's not clearly evident from micrograph presented in Fig. 1b. However, the surface of treated cenospheres appears to be better and smooth as compared to untreated ones (Fig. 1a). Particle size analysis and FTIR of untreated and treated fly ash cenospheres confirm the presence of silane as reported in Ref. [24,45]. These treated cenospheres are expected to improve the overall properties of the foams due to the better bonding of constituent materials. The manual stirring approach is used to cast cenosphere/epoxy syntactic foams. Uniform dispersion with minimum particle failure of cenospheres in matrix resin is a challenging task. However, micrographs of as-cast fractured E60-U and E60-T foams (Fig. 2a and Fig. 2c) show uniform dispersion of cenospheres within the epoxy matrix, justifying manual stirring method for casting the syntactic foams. E60-U foams show poor interfacial bonding (Fig. 2b) while E60-T foams exhibit better bonding between the constituents (Fig. 2d). Density, void content estimation and weight saving potentials of syntactic foams are

Table 2
Wear parameters used in the present investigation [32,64].

Input parameters		Output parameters
Cenosphere content, (vol %)	0, 20, 40 and 60	Wear rate (mm^3/km)
Cenosphere morphology	Untreated and treated	Specific Wear rate (mm^3/km-N)
Load, F (N)	30 and 50	Coefficient of friction
Sliding velocity, V (m/s)	2 and 5	Temperature (°C)
Sliding distance, D (km)	3, 5 and 7	

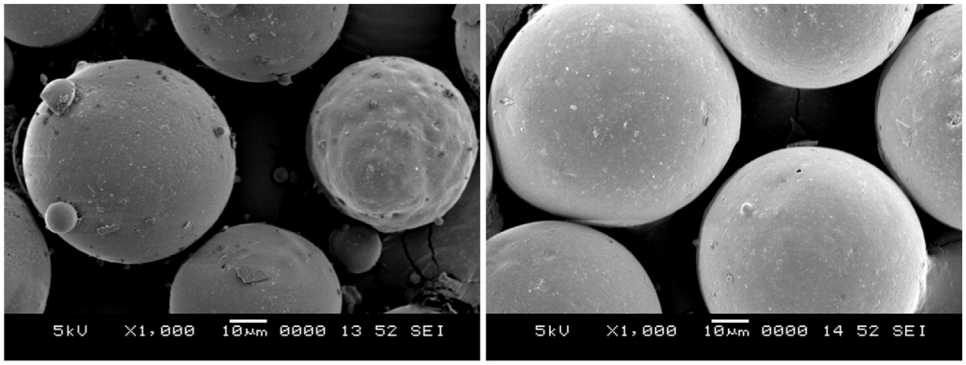

Fig. 1. Micrographs of (a) as received and (b) silane modified cenospheres.

listed in Table 3 [24]. Density reduction of samples is attributed to more number of hollow cenospheres embedment into the matrix resin. Untreated syntactic foams reveal 14% reduction in density as compared to neat epoxy, whereas surface modified syntactic foams register higher density owing to silane coating. Air entrapment in the matrix during mechanical mixing of cenospheres in the epoxy matrix has reduced the experimental density as compared to the theoretical values. Matrix void content is noted to increase with increasing filler loading except E60 (Table 3). Small variations are observed in standard deviations affirming the uniformity in sample processing.

Fig. 3 presents a typical set of wear test results. Height loss (Fig. 3a) and frictional force (Fig. 3b) are graphed against sliding speed. These representative results are obtained on neat epoxy, E60-U and E60-T samples for $V_2F_{50}D_3$ conditions. For neat epoxy samples, the wear attains a steady state after an initial transition period as observed in Fig. 3a. A similar trend is demonstrated by E60-U and E60-T foams as seen from this figure, although the transient region is less pronounced.

Table 3
Density and matrix void fraction in syntactic foams [24].

Material	ρ^{th} (kg/m^3)	ρ^{exp} (kg/m^3)	Φ_v (%)	Weight saving potential with E
E0	–	1192.00 ± 23.84	0.34	–
E20-U	1137.60	1129.63 ± 22.59	0.70	5.23
E40-U	1083.20	1064.72 ± 21.29	1.71	10.68
E60-U	1028.80	1028.36 ± 20.56	0.05	13.73
E20-T	1153.60	1133.14 ± 22.66	1.78	4.94
E40-T	1115.20	1073.92 ± 21.47	3.70	9.91
E60-T	1076.80	1055.65 ± 21.11	1.98	11.44

Further, height loss in neat resin specimens is twice as that of syntactic foam specimens at 1500 m as observed in Fig. 3a. This observation implies that the cenospheres in epoxy resin enhance wear resistance. Further, the frictional force of syntactic foams is low compared to the

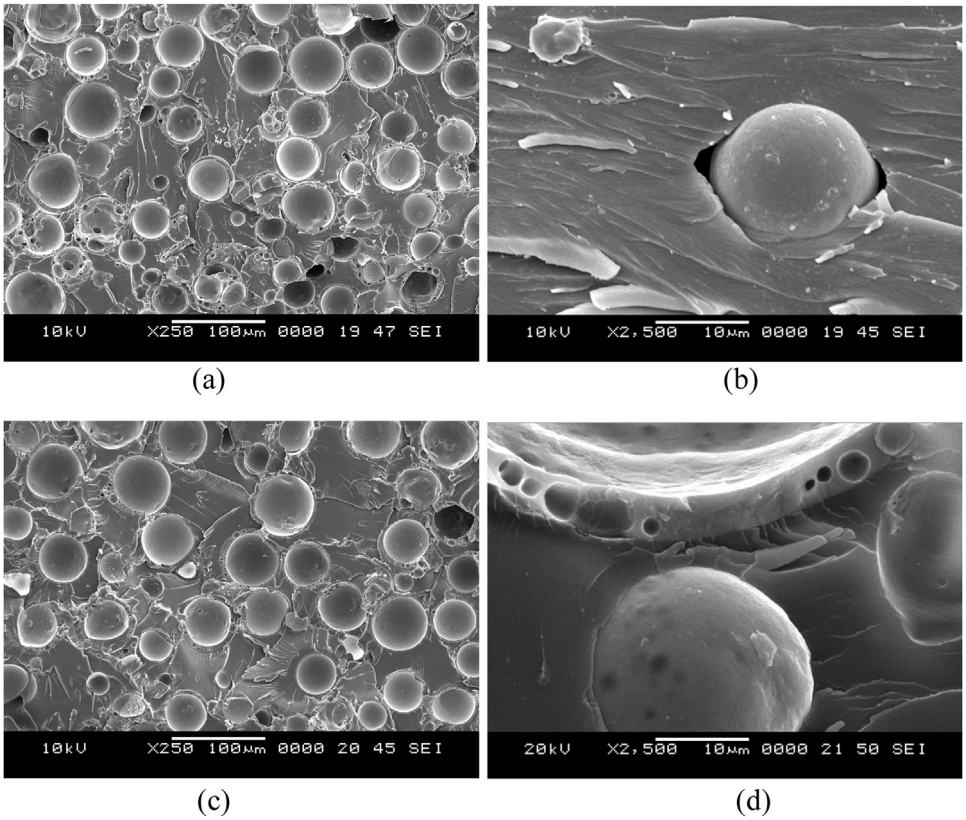

Fig. 2. As cast fractured E60-U at (a) lower (b) higher magnification and E60-T at (c) lower (d) higher magnification.

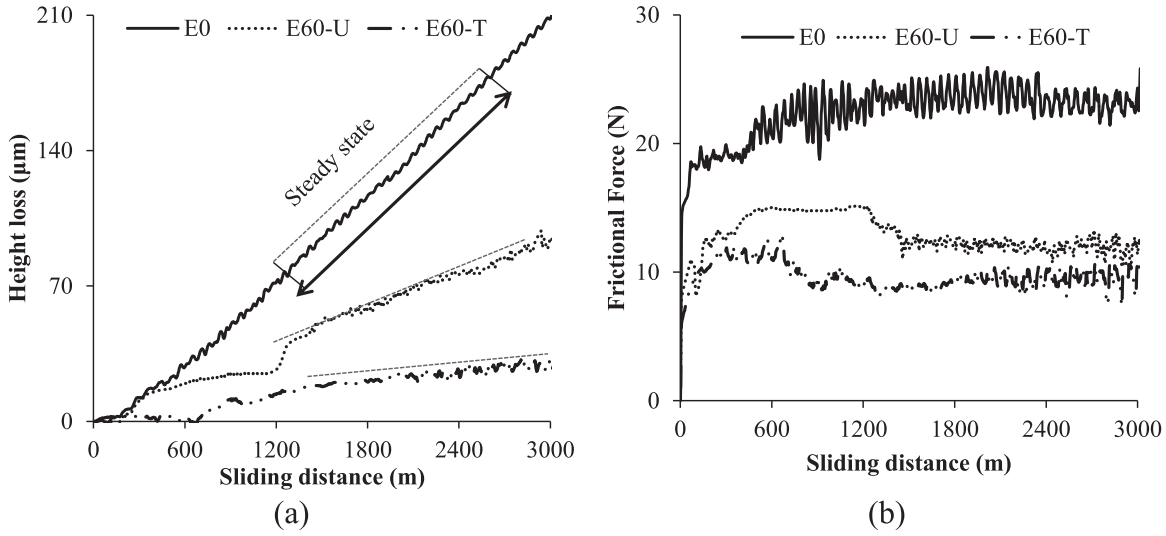

Fig. 3. Typical graphs of the wear test (a) height loss and (b) frictional force with respect to the sliding speed of wear.

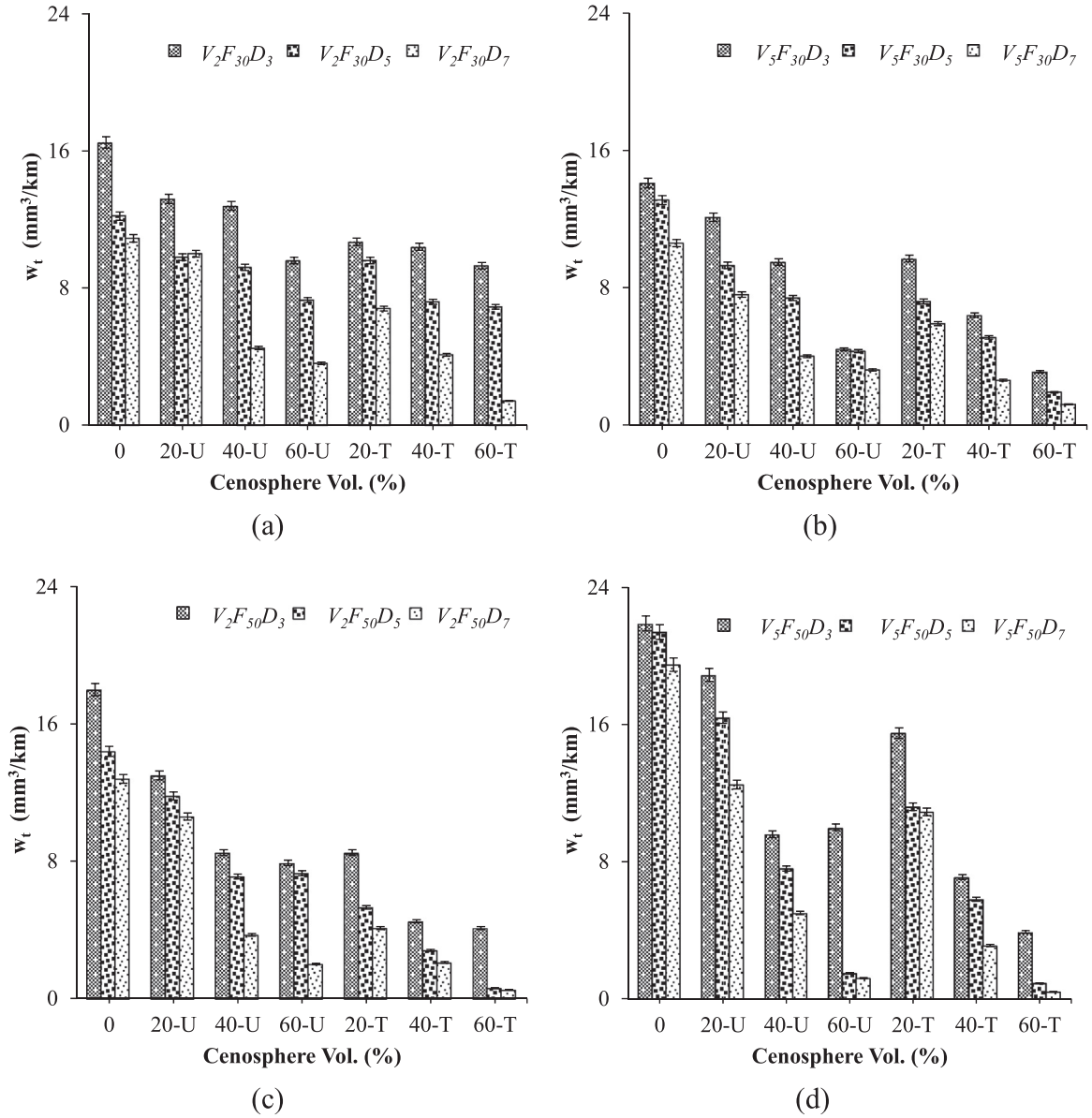

Fig. 4. Plots of w_t for different filler contents (a) V_2F_{30} (b) V_5F_{30} (c) V_2F_{50} and (d) V_5F_{50}. Error bars represent the standard deviation of the data.

neat resin samples. All the samples attain a steady state frictional force with increase in sliding speed. For the same sliding speed, the frictional force in E60-U and E60-T syntactic foam specimen reduces by 55% and 71% respectively as compared to the neat resin highlighting the effectiveness of cenospheres in these syntactic foams for tribological applications. The fluctuations observed in Fig. 3 are attributed to the sudden opening up of the cenosphere void space after filler breakage during the test and presence of wear debris between the sliding surfaces.

3.2. Wear rate (w_t)

Wear rate is found to decrease with increase in sliding velocity for 30 N loading whereas an increase is noted for the 50 N load (Fig. 4). Further, it is noted that w_t shows a declining trend with increasing filler loading and sliding distances. Neat epoxy reveals the highest w_t as compared to EXX-U and EXX-T foams for all the tested conditions. Increase in the applied load increases w_t for neat epoxy samples and foams with lower filler contents (E20) whereas decrease with increasing cenospheres signifies the advantage of having higher filler contents in an epoxy matrix. w_t for treated syntactic foams is better as compared to EXX-U and E0 under all the tested conditions. Maximum w_t of 21.9, 18.9 and 15.5 mm^3/km for neat epoxy, E20-U, and E20-T foams respectively are observed at $V_5F_{50}D_3$.

In case of V_2F_{30} test condition, w_t is maximum for neat epoxy samples. Further, it is observed that the addition of cenospheres into the matrix decreases w_t (Fig. 4a). Primary constituents of cenospheres are aluminum and silica. These cenosphere particles are broken into fine fragments and get mixed with the matrix resin constituting debris [14]. Combination of brittle aluminum and silica particles with epoxy matrix resist the wear of syntactic foams. Increasing the filler content further ensures better wear resistance. Fig. 4a reveals that w_t decreases with an increase in sliding distance for all the samples. Lower sliding distances (D_3) provide higher w_t as compared to D_7. The surface of both epoxy and cenospheres gets smoothened as the wear progresses reducing wear further. Deviation in w_t with an increase in D is attributed to changes in the surface roughness, surface chemistry and effective contact area [52]. Abrasive mode of wear mechanism is observed for these conditions.

At V_5F_{30} condition, w_t decreases with an increase in sliding velocity for all the samples (Fig. 4b). Frictional heating is very low at an applied load of 30 N. As a result, w_t of the neat epoxy sample decreases slightly. On the other hand, the nominal contact surface between syntactic foams and the disc reduces, owing to the microballoons void space opening post fracture. Under lower applied load (F_{30}), wear debris does not get compacted in the void spaces effectively resulting in marginal variation of wear rate as velocity increases.

For V_2F_{50} condition, w_t decreases with increasing load from 30 to 50 N for syntactic foam samples (Fig. 4c) whereas w_t increases for neat epoxy. Volume loss of epoxy based composites generally increases with the rise in sliding speed and applied load [53]. For neat epoxy samples at F_{50}, load distribution across the overall asperities increases. These asperities pierce deeper into the matrix surface registering higher w_t [54]. However, syntactic foams show a decrease in w_t owing to the presence of a higher volume of cenospheres (Fig. 4c). These hard shell particles of cenospheres are effective in reducing w_t by preventing matrix damage over a greater scale. Lower contents of the matrix in E40 and E60 samples reduce the wear rate considerably as compared to E20. Higher load reduces surface asperities effectively. The transition from abrasive to the adhesive mode of wear mechanism is observed for V_2F_{50}.

At V_5F_{50} condition, w_t increases significantly for neat epoxy samples owing to high frictional forces generated at the interface whereas w_t decreases for EXX-U and EXX-T foams due to the better resistance offered by the cenosphere particles (Fig. 4d). For neat epoxy samples, the surface is severely strained and wear debris tends to adhere to the disc. The size of this neat epoxy debris is larger, exhibiting undulations in w_t. On the contrary, for EXX-U and EXX-T foams, the debris generated is smaller in size and gets accumulated at the craters of broken cenosphere sites. Small amounts of wear debris that lie on the surface facilitate better plastic flow making the surface relatively smoother. Increase in filler loading provides more void spaces for debris accumulation, reducing w_t further. Increase in applied load creates a localized fusion of broken cenosphere fragments leading to a high degree of adhesive wear. As a result, adhesive mode of wear mechanism is prominent for the V_5F_{50} condition. These events lower w_t in syntactic foams.

For EXX-U and EXX-T foams, w_t decreases in the range of 8–94% and 21–98% respectively, compared to neat epoxy for all the tested conditions. E20 poses fewer void spaces for wear debris accumulation as compared to E40 and E60. Further, the behavior of E20 is matrix dominated. Thereby, E20 samples register higher w_t. Significant reduction in w_t is achieved with an increase in the cenosphere content (E60) owing to higher space availability for accommodating wear debris. Epoxy matrix being the softer phase compared to cenospheres, the wear resistance of the matrix is very low. Embedding more number of cenospheres in matrix considerably enhances overall wear resistance of the syntactic foam. However, for all the filler contents, EXX-T foams show a lower w_t compared to EXX-U. As compared to EXX-U foams, wear rate in EXX-T foams decreases in the range of 2–92%. Lower resistance of EXX-U foams is due to poor interfacial adhesion between the constituents (Fig. 2b). While in the case of EXX-T, good interfacial bonding (Fig. 2d) resists the material removal for longer contact time before finally wearing out resulting in reduced w_t. Weaker interfacial adhesion between cenospheres and epoxy resin in EXX-U easily initiates cracks at the interfacial region under the applied load. As a result, the matrix resin is easy to rub-off without the effective reinforcement of

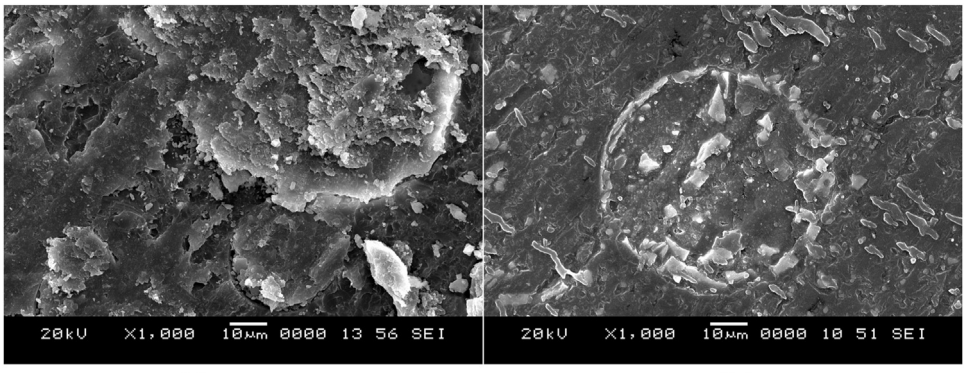

Fig. 5. Micrograph of post wear test of (a) E20-U and (b) E20-T foams.

cenosphere in friction, leading to the rough worn surface, higher friction coefficient and wear rate. Poor interfacial bonding between the constituents in EXX-U results in cenospheres getting dislodged easily with scuffing of the counterpart surface leading to higher wear. For EXX-T foams, due to the enhancement of constituent materials bonding, cenospheres strongly adhered to the matrix. During the wear test, surface modified cenospheres carry most of the load. Thereby, direct contact and adhesion between the matrix and the counterpart are reduced leading to lower friction coefficient and smoother worn surface. With the strong bonding between cenosphere and the matrix, the fillers cannot be easily dislodged from the matrix under the applied load. The load-carrying ability of the foam is thus improved restraining large-scale shedding and rubbing-off of epoxy matrix reducing w_t. Fig. 5 present micrographs of post wear test of E20-U and E20-T foams. Void spaces are seen to be completely filled for both E20-U and E20-T foams as seen in Fig. 5. Further, it's clearly evident that effective compaction of wear debris is seen in E20-T (Fig. 5b) as compared to untreated filler (Fig. 5a). Additionally, worn out surface is observed to be smoother (Fig. 5b) in the surface modified filler reinforced epoxy matrix. Such occurrences enhance the wear resistance of EXX-T foams as compared to EXX-U foams.

3.3. Specific wear rate (w_s)

Specific wear rate of neat epoxy and their syntactic foams are presented in Fig. 6. Effect of D and filler loading on the w_s at V_2F_{30} condition is presented in Fig. 6a. In line with w_t, w_s of all syntactic foams decreases with increase in D and cenosphere content (Fig. 6). It is further observed from Fig. 6b that as the applied load is increased to 50 N, w_s decreases substantially for all the compositions demonstrating enhanced wear resistance at higher loads [55,56]. EXX-T foams reveal the highest resistance among all the compositions. The higher resistance offered by treated syntactic foams to wear can be solely due to the strong bonding exhibited between the constituents making them potential materials in dry sliding wear environments. Further, similar trends are observed with an increase in sliding velocity (Fig. 6c and Fig. 6d). Fig. 6 reveals that E60 exhibited minimum w_s from all the test conditions. The combined effect of higher sliding velocity and applied load is beneficial in reducing the specific wear rate [32]. At higher sliding velocity and applied load, the transfer film is formed easily

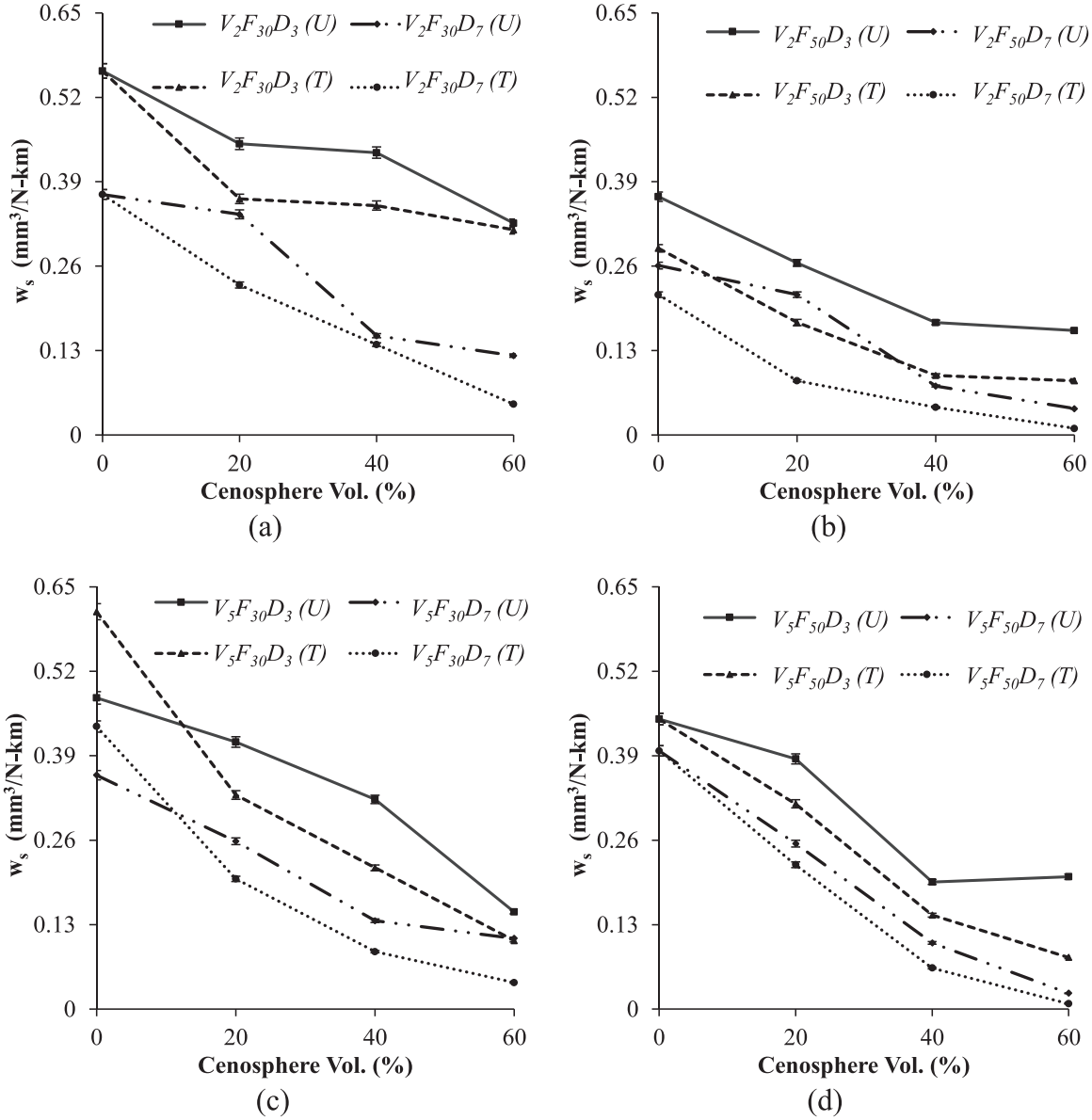

Fig. 6. Plots of w_s for different filler contents at (a) V_2F_{30} (b) V_2F_{50} (c) V_5F_{30} and (d) V_5F_{50}.

which is difficult to rupture for EXX-U and EXX-T foams due to the adhesive mechanism, resulting in better wear resistance as compared to neat epoxy. In E60, cenospheres are available in higher numbers as compared to E20. Higher particles on worn surface result in the higher contact area. As a result, the resistance offered with higher filler contents of cenospheres is much better. EXX-T foam with E60 has minimum w_s among all the sample compositions. E60-T foam has minimum w_s of 0.0082 mm^3/N-km and maximum w_s of 0.5607 mm^3/N-km is observed for neat epoxy samples.

3.4. Coefficient of friction (μ)

Variation of μ for different study parameters is presented in Fig. 7. Neat epoxy presents the highest μ compared to EXX-U and EXX-T foams. It is seen from Fig. 7a, that with V_2F_{30}, μ decreases with increase in cenosphere content. As filler loading increases, fragmented cenospheres coming into contact with the counter surface are more, resulting in lower data fluctuations leading to lower values of surface roughness and μ. The values of μ vary in the range of 0.20–0.55. It is noted in Fig. 7b that, μ values are significantly reduced at F_{50} as compared to F_{30} [57]. It is attributed to the increase in frictional heat at the interface which leads to lubricating film formation on the worn surface. Thereby, the flow-ability increases and causes slip phenomena. In addition to this, wear debris get easily accumulated within the void space of broken cenospheres making the surface still smoother. The values of μ vary in the range of 0.19–0.6 for the testing condition of V_2F_{50}. With the increase in sliding velocity, μ increases (Fig. 7c) owing to higher shear force. These shear forces lead to temperature rise at the interface of sample and disc resulting in increased thermal penetration from disc towards the test samples. As a result, the bond across the filler-matrix interface weakens. Consequently, cenosphere particles get dislodged easily and shear away owing to axial thrust, increasing μ. The values of μ are seen to be varying in the range of 0.38–0.59 for V_5F_{30}. Similar to Fig. 7b, with an increase in F and V, μ decreases as observed in Fig. 7d. As mentioned earlier, the combination of an increase in temperature and shearing forces at the interface results in a marginal decrease of μ. The values of μ vary in the range of 0.30–0.63 in V_5F_{50}. Further, it is observed that μ increases with increase in D for all the tested conditions. Therefore, it can be concluded that μ is a strong function of V and D. With the increase in V and D, μ for syntactic foams increases while it decreases with increasing cenosphere content and F.

3.5. Temperature rise (T)

The variation of disc temperature for minimum and maximum conditions of sliding velocity and applied load are presented in Fig. 8. At V_2F_{30} condition, the temperature increases with an increase in D wherein low adiabatic heating takes place (Fig. 8a). It is further noted that the temperature decreases with increase in filler loading. It is attributed to reduced undulations of samples owing to the presence of

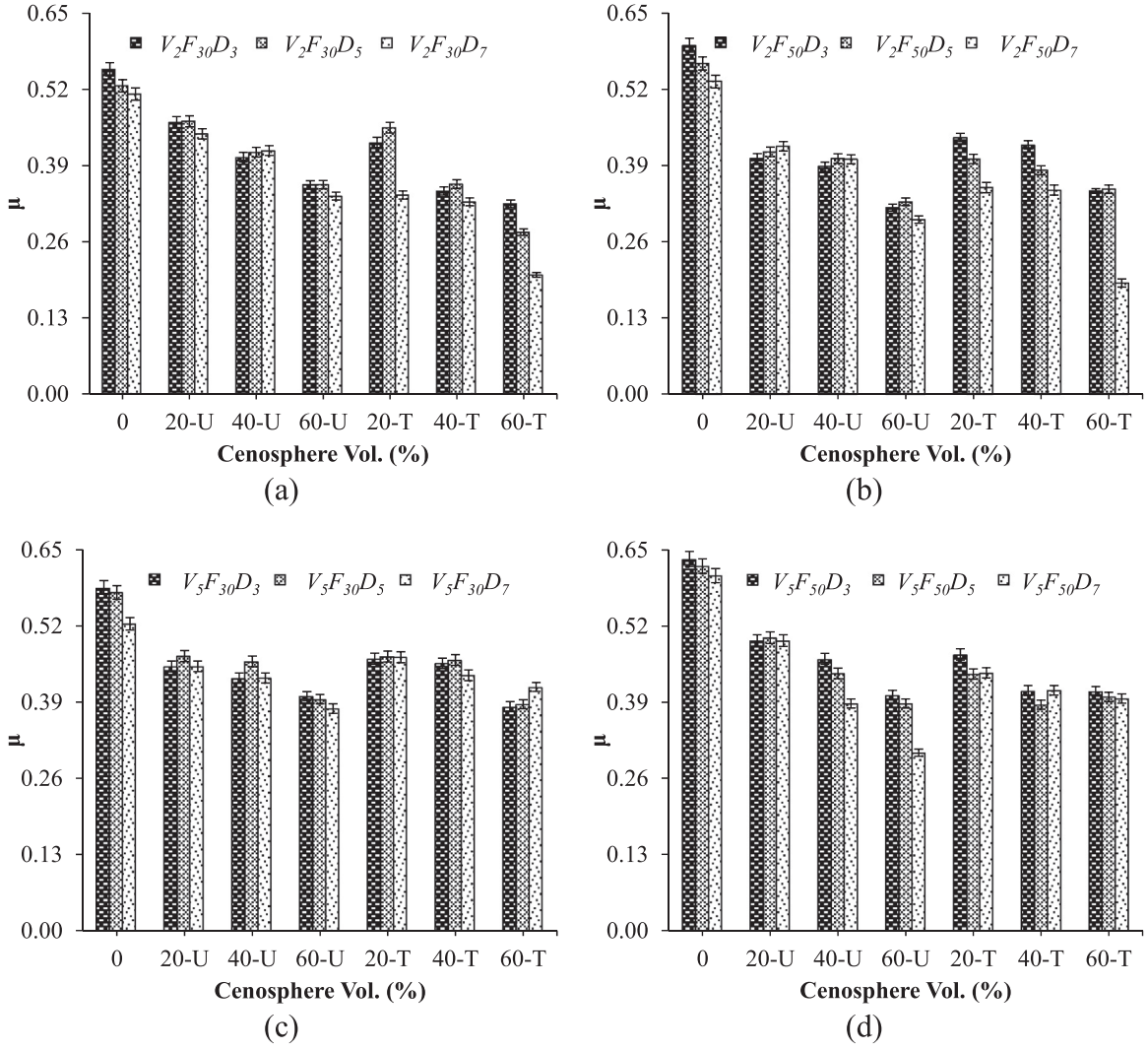

Fig. 7. Plots of μ for different filler contents at (a) V_2F_{30} (b) V_2F_{50} (c) V_5F_{30} and (d) V_5F_{50}. Error bars represent the standard deviation of the data.

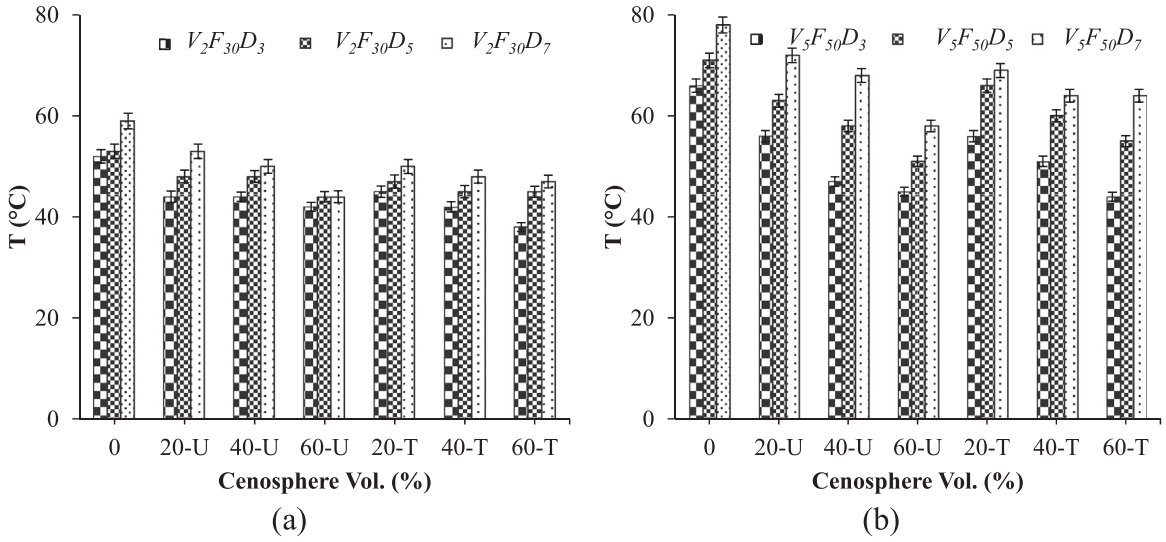

Fig. 8. Plots of temperature with respect to filler content for (a) V_2F_{30} and (b) V_5F_{50}. Error bars represent the standard deviation of the data.

cenosphere particles. Further, increase in interconnected spaces between the cenosphere particles results in a higher effective surface area. The absence of such hollow cenospheres in neat epoxy samples registers the highest temperature. EXX-T foams registered lowest disc temperature as compared to EXX-U foams. The rise in temperature is significant for V_5F_{50} conditions (Fig. 8b). This is due to the combination of high frictional forces and increased adiabatic heating at the interface. Temperature rise is seen to be a strong function of *V*, *F* and *D*. Irrespective of *V* and *F*, the temperature decreases with the increase in cenosphere content.

3.6. Wear debris analysis

Elemental composition of debris analyzed by EDS is presented in Table 4. The elements found in wear debris are aluminum, silica, iron, carbon, and oxygen. Aluminum and silica present in the debris are the primary constituents of cenospheres. These hard elements are effective in minimizing wear. Significant wear resistance is achieved with an increase in cenosphere content (presence of aluminum and silica). Presence of iron in the wear debris is mainly from the disc counterpart (EN 31 steel). For E20, the rough worn surfaces of the foams and discontinuous transfer films on counter faces result in a large number of iron particles transferred from EN 31 steel disc to the worn surfaces of the foams. In E60, the amount of iron content in the wear debris decreases due to the presence of transfer film. For EXX-T foams, smooth worn surface and uniform transfer film on counter face effectively reduce the wear of the counterpart further. Thereby, small traces of iron are observed as compared to EXX-U foams (Table 4). The content of carbon and oxygen in the debris are very high implying debris is constituted primarily of epoxy resin. Micrographs of wear debris post wear test for all the samples are presented in Fig. 9. The wear debris chunks are seen to be much larger for neat epoxy (Fig. 9a) as compared to syntactic foams (Fig. 9b-e). During the wear test, material removal for neat epoxy is in the form of large chunks owing to the brittle behavior of the matrix and the high frictional force caused therein (Fig. 9a). With higher filler loading wear debris chunk size decreases and smaller size cenosphere fragments combine with a matrix to form wear debris. The lower amount of filler content provides a limited source of broken cenosphere fragments to be part of the wear debris. As a result, the size and shape of the debris at E20 is governed by the epoxy matrix (Fig. 9b and Fig. 9c). At E60, a large amount of fragmented cenosphere particles availability and lower matrix content decreases the wear debris size (Fig. 9d and Fig. 9e) as compared to neat epoxy and foams with lower filler contents. However, it is observed from Fig. 9c and Fig. 9e (EXX-T) that the size of the wear debris is considerably smaller as compared to neat epoxy and EXX-U foams. This is attributed to the constrained source of finely fragmented cenospheres particles and matrix from the wear surface owing to better bonding between the constituents.

3.7. Wear surface analysis

Micrographs of worn-out samples under lower operating conditions (V_2F_{30}) are presented in Fig. 10. On the surface of the neat epoxy sample, grooves having larger width are visible in the sliding direction. These grooves increase wear rate owing to material removal (wear debris). For E20, matrix dominates the wear behavior. A closer observation of worn out surface in Fig. 10c reveals fine grooves on the EXX-T foam surface and material flow along the sliding direction. These grooves are primarily due to the discontinuity created at the cenosphere-epoxy interface due to the presence of cenosphere wall in the sliding direction. Similar observations are observed for EXX-U foam (Fig. 10b). As the wear debris approaches the craters of partially broken cenosphere sites, they tend to fill the void space. At the same time, inadequate compaction of wear debris at the surface of the broken cenosphere due to lower applied load leads to initiation of small grooves post cenosphere wall in the sliding direction. Due to series of such events, w_t increases at lower filler contents primarily indicating the dominance of abrasive wear mechanism at lower cenosphere content. A similar type of worn surface is also noted for E60-U and E60-T samples (Fig. 10d and Fig. 10e). The discontinuities in the form of grooves are observed again at the cenospheres location having a lower scale as compared to E20 syntactic foam. A matrix being the relatively softer phase tends to deteriorate far more easily as compared to filler. Addition of higher filler in the matrix effectively reduces wear of the syntactic foams [32]. As a result, the discontinuities at the cenosphere locations decrease for E60 samples owing to the fact that with an increase in filler loading matrix content reduces. Thereby, w_t decreases at higher filler contents. It is clearly evident from these observations that

Table 4
Elemental composition of the wear debris.

Composition (wt%)	E0	E20-U	E20-T	E60-U	E60-T
Carbon	64.65	59.95	68.63	64.57	62.82
Oxygen	22.78	22.51	21.56	21.28	23.23
Silicon	–	4.81	1.78	5.20	6.22
Aluminum	–	2.97	0.47	3.35	2.82
Iron	12.57	9.76	7.56	5.60	4.91

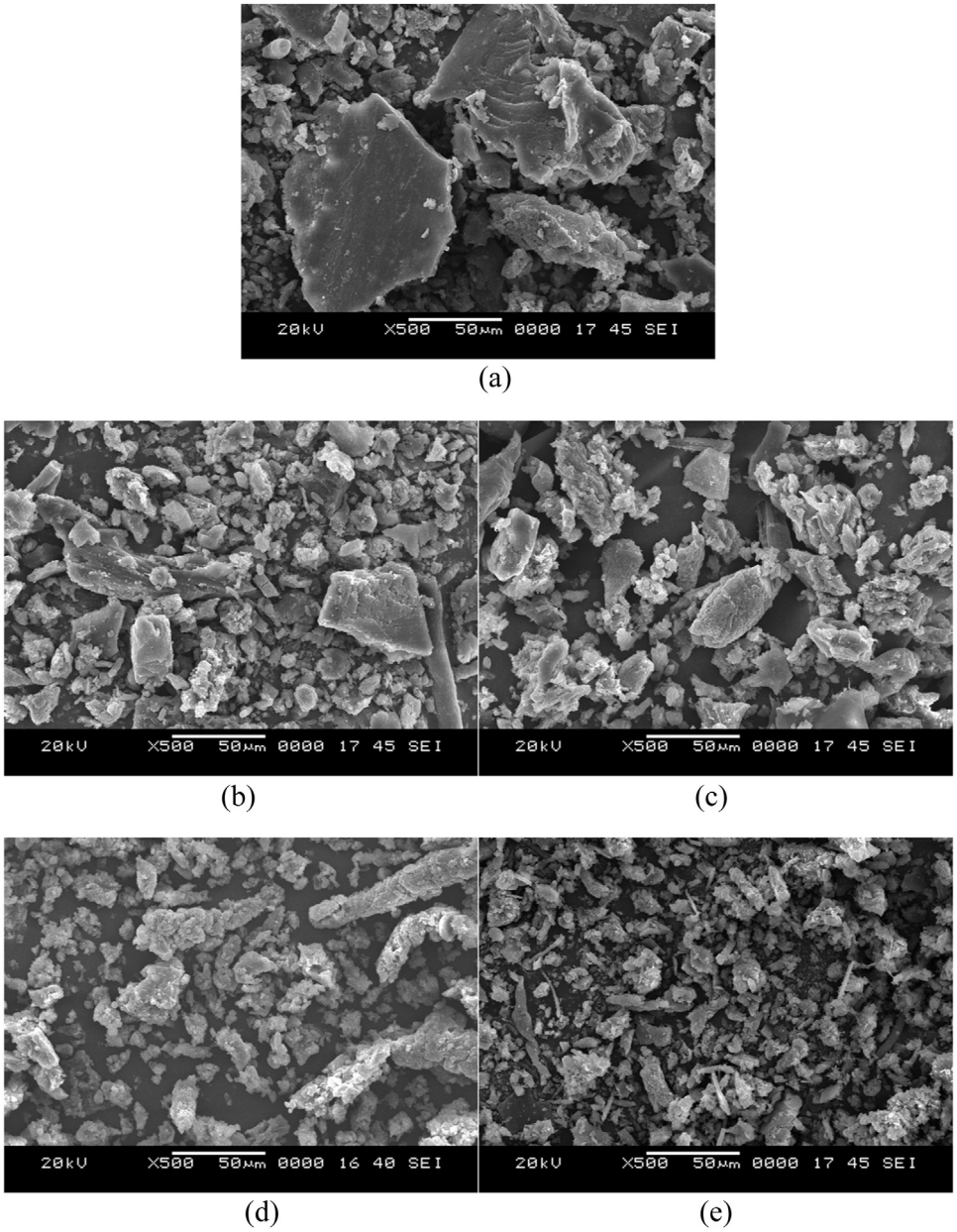

Fig. 9. Wear debris micrographs of (a) E0 (b) E20-U (c) E20-T (d) E60-U (e) E60-T samples.

wear behavior is greatly influenced by the filler content in the syntactic foam.

Post wear test, micrographs of the worn-out surface of samples at V_5F_{50} conditions are presented in Fig. 11. Increasing load increases the possibility of wear debris being smeared along the sliding direction with greater extent of material flow for neat epoxy samples (Fig. 11a). Plucked and plowed marks appear all along the sliding direction of the neat sample confirming higher wear rate. Wear response of E20-U and E20-T foams are presented in Fig. 11b and Fig. 11c respectively. A closer observation reveals that the debris is slithered at the disc-sample interface and gets entrapped in void space of the partially broken cenosphere. Further, a higher amount of compacted wear debris gets detached (combined action of localized fusion and weak bonding between constituents) from the cenosphere craters in EXX-U is clearly visible (Fig. 11b). These observations indicate that the combined effect of high velocity and applied load increases the shearing force and softens wear debris substantially by plastic deformation [14]. As a result wear rate is higher for E20.

Wear rate reduces significantly for E60 as compared to E0. This is due to the presence of more cenosphere particles in the matrix. Formation of wear debris and transfer film is very high owing to more fragmented particles of cenospheres at higher filler loadings [58]. At higher sliding velocity and applied load, the possibility of transfer film formation from wear debris is higher leading to reduced wear as compared to lower filler contents. Moreover, higher loads normalize the surface asperities and thereby exhibit a more stable w_t [32]. The distance to reach steady state decreases with increasing load. In addition to this, the resistance offered by the hard shells of cenospheres that are primarily made up of alumina silicates also help in reducing w_t further. Debris accumulated in the broken cenospheres are very well compacted at higher sliding velocity and applied load as seen in Fig. 11e. Such an effective compaction leads to reduced fluctuations, lowering w_t significantly. From the micrographs presented in Fig. 10, it is clearly evident that at lower operating conditions, w_t is higher due to initiation of fine grooves along the sliding direction. As filler loading increases, w_t decreases due to a reduction in the magnitude and number of grooves

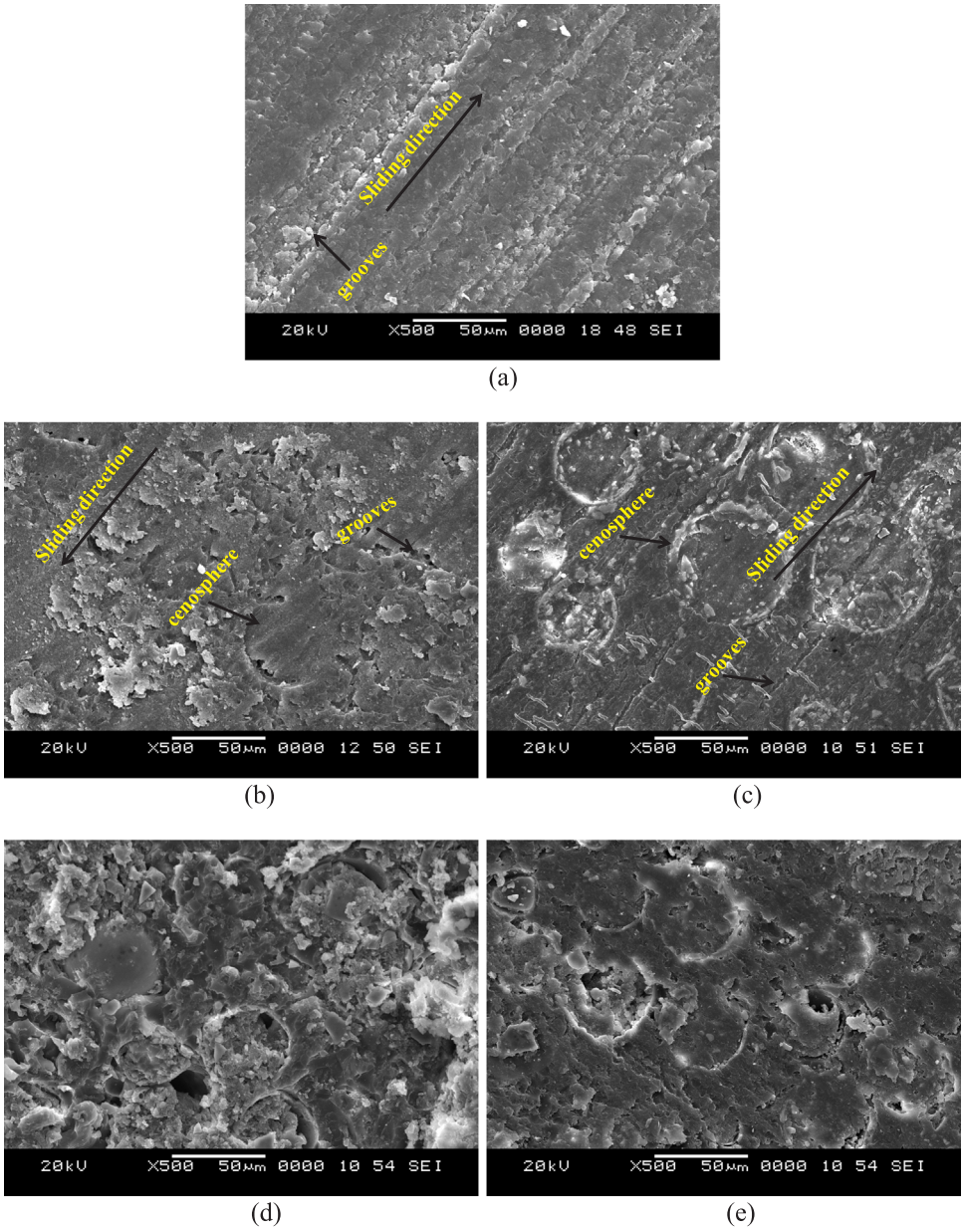

Fig. 10. Micrographs of worn-out surface of (a) E0 (b) E20-U (c) E20-T (d) E60-U (e) E60-T at V_2F_{30}.

because of lower matrix content. Abrasive or plowing mode of wear mechanism is observed from these micrographs. At higher operating conditions (Fig. 11), w_t decreases with increase in cenosphere content due to the increase in frictional heat which helps in thin film formation. Surface modification of cenospheres has effectively reduced the wear rate by providing effective transfer film and better compaction of wear debris. E60-T is best suited for dry sliding wear applications with weight saving potential of around 12% as presented through this study.

3.8. Property map

Property map is presented in this section which comes in handy and acts as a guideline for industries in choosing the specific composition based on the envisaged application. Results presented in this work and the data extracted from the available literature are graphed as a function of density for comparative analysis [14,34,59–63] (Fig. 12). Standard deviations are plotted for the wear plots attained in the present study. However, the values extracted from the literature to plot the property map are average values and therefore no standard deviations are reported for the results excluding the present work. It is clearly evident from the figure that polymer composites with higher density exhibit higher wear rates. However, the advantage of hollow cenospheres filled lightweight syntactic foams is clearly seen from Fig. 12. In the present study, the density of all the syntactic foams including neat epoxy is lower than the other composites investigated in the literature. Syntactic foams outperform alkali treated, sea water treated, sugar palm fiber reinforced phenolic resin composites and vinylester/cenosphere composites. Wear rates are lower at higher filler contents of cenospheres (E60) as seen in Fig. 12. Additionally, data extracted from metal matrix composites are presented in the property map. E60-T foam reveals the lowest wear rate whereas E60-U foam presents the lowest density and outperforms metal matrix composites with rice husk ash, fly ash and silicon carbide particles. Therefore, from the property map, it can be concluded that cenosphere/epoxy syntactic foams with higher cenosphere contents provide lower wear rates and density as compared to the other composites signifying their suitability in weight sensitive applications in wear regime. Abundant availability of environment pollutant fly ash cenospheres can be thus effectively utilized to prepare

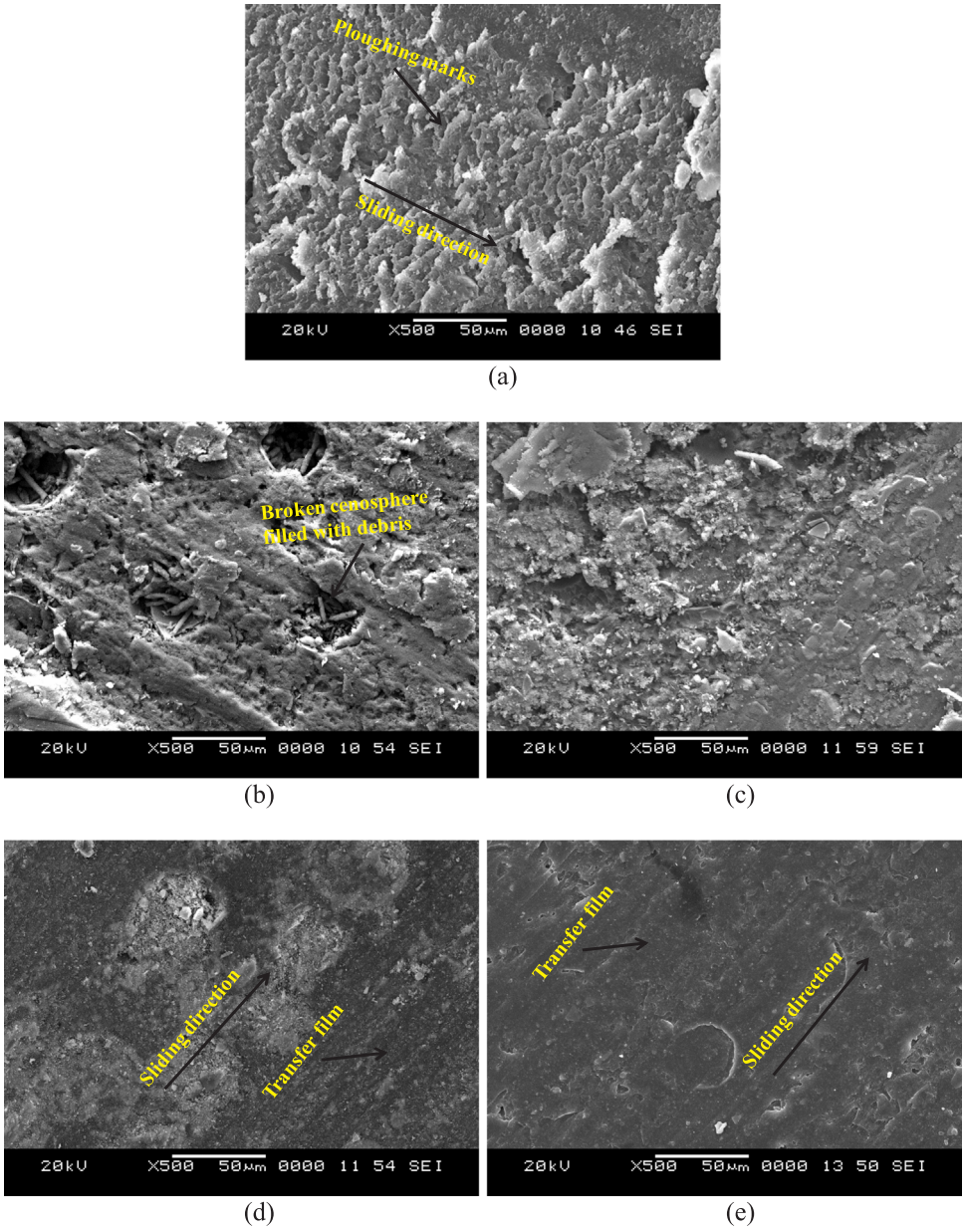

Fig. 11. Post wear test micrographs of (a) E0 (b) E20-U (c) E20-T (d) E60-U (e) E60-T samples at V_5F_{50}.

foams for various applications demanding lightweight and wear resistance properties.

4. Conclusions

Dry sliding wear of cenosphere/epoxy syntactic foams targeted for brake pad applications is investigated for varying velocity, applied load and sliding distance against EN31 steel disc. Effect of filler loading and surface treatment as a function of wear test parameters are presented in this work. Following conclusions are drawn:

- Maximum wear is registered by neat epoxy samples. Wear rate decreases with increasing filler content of cenospheres for EXX-U and EXX-T foams.
- Compared to neat epoxy, wear resistance of EXX-U and EXX-T foams increases in the range of 8–94% and 21–98% respectively.
- Silane treatment of cenospheres has increased the wear resistance of EXX-T foams and is in the range of 2–92% as compared to EXX-U foams. E60-T foams exhibit the highest dry sliding wear resistance among all the samples.
- Specific wear rate of syntactic foams decreases significantly at higher applied loads. EXX-T foams are best suited for wear environments owing to good bonding between the constituents.
- Coefficient of friction decreases with increase in cenosphere content and sliding distance.
- Wear debris of neat epoxy samples is larger in size as compared to EXX-U and EXX-T foams.
- Micrographs of worn out surface reveal that for lower operating conditions, w_t is higher due to initiation of fine grooves along the sliding direction. As cenosphere content increases, w_t decreases.
- Abrasive mode of wear mechanism is observed in V_2F_{30}. At higher operating conditions, w_t decreases with increase in filler loading. Higher frictional heat in formation of thin films and better compaction of wear debris within the cenospheres contribute in reducing the wear for E60-T foams.
- Transition from abrasive to the adhesive mode of wear mechanism is observed for V_5F_{50} for all the samples under investigation.
- Property map reveals cenosphere/epoxy syntactic foams exhibit

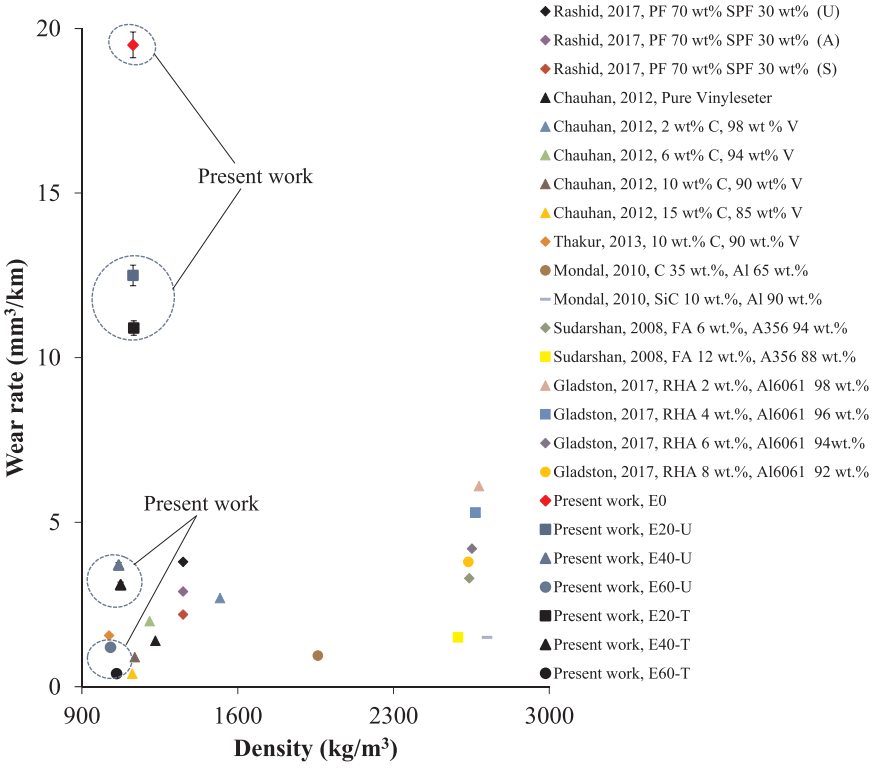

Fig. 12. Wear rate plotted against density from available studies [14,34,59–63]. Note: PF – Phenolic resin, SPF – Sugar Palm Fiber, U – Untreated, A – Alkali treated, S – Seawater treated, C - Cenosphere, V – Vinylester, RHA – Rice Husk Ash, FA – Fly Ash, SiC – Silicon Carbide, Al – Aluminum, A356 – Aluminum silicon alloy, Al6061 – Hardened aluminum alloy.

lowest wear rates at higher cenosphere contents as compared to other composites signifying their suitability in weight sensitive applications subjected to dry sliding wear scenario.

Acknowledgment

Author Mrityunjay Doddamani acknowledges DST grant DST/TSG/AMT/2015/394/G by Govt. of India. The authors would like to thank the ME Department at NIT-K for providing facilities and support.

References

[1] N. Gupta, S.E. Zeltmann, V.C. Shunmugasamy, D. Pinisetty, Applications of polymer matrix syntactic foams, JOM 66 (2) (2014) 245–254.
[2] M.L. Jayavardhan, B.R. Bharath Kumar, M. Doddamani, A.K. Singh, S.E. Zeltmann, N. Gupta, Development of glass microballoon/HDPE syntactic foams by compression molding, Compos. Part B: Eng. 130 (Suppl. C) (2017) S119–S131.
[3] N. Gupta, D. Pinisetty, V.C. Shunmugasamy, Reinforced Polymer Matrix Syntactic Foams: Effect of Nano and Micro-Scale Reinforcement, Springer International Publishing, Cham, 2013.
[4] V. Manakari, G. Parande, M. Doddamani, M. Gupta, Enhancing the ignition, hardness and compressive response of magnesium by reinforcing with hollow glass microballoons, Materials 10 (9) (2017) 997.
[5] D.D. Luong, O.M. Strbik III, V.H. Hammond, N. Gupta, K. Cho, Development of high performance lightweight aluminum alloy/SiC hollow sphere syntactic foams and compressive characterization at quasi-static and high strain rates, J. Alloy. Compd. 550 (2013) 412–422.
[6] A.K. Singh, B. Patil, N. Hoffmann, B. Saltonstall, M. Doddamani, N. Gupta, Additive manufacturing of syntactic foams: Part 1: development, properties, and recycling potential of filaments, JOM 70 (3) (2018) 303–309.
[7] A.K. Singh, B. Saltonstall, B. Patil, N. Hoffmann, M. Doddamani, N. Gupta, Additive manufacturing of syntactic foams: Part 2: specimen printing and mechanical property characterization, JOM 70 (3) (2018) 310–314.
[8] N. Gupta, B. Singh Brar, E. Woldesenbet, Effect of filler addition on the compressive and impact properties of glass fibre reinforced epoxy, Bull. Mater. Sci. 24 (2) (2001) 219–223.
[9] P.K. Rohatgi, D. Weiss, N. Gupta, Applications of fly ash in synthesizing low-cost MMCs for automotive and other applications, JOM 58 (11) (2006) 71–76.
[10] M. Doddamani, S.M. Kulkarni, Dynamic response of fly ash reinforced functionally graded rubber composite sandwiches-a Taguchi approach, Int. J. Eng. Sci. Technol. 3 (1) (2011) 17.
[11] J. Li, A. Agarwal, S.M. Iveson, A. Kiani, J. Dickinson, J. Zhou, K.P. Galvin, Recovery and concentration of buoyant cenospheres using an Inverted Reflux Classifier, Fuel Process. Technol. 123 (2014) 127–139.
[12] R.J. Lauf, Cenospheres in fly ash and conditions favouring their formation, Fuel 60 (12) (1981) 1177–1179.
[13] N.N. Anshits, O.A. Mikhailova, A.N. Salanov, A.G. Anshits, Chemical composition and structure of the shell of fly ash non-perforated cenospheres produced from the combustion of the Kuznetsk coal (Russia), Fuel 89 (8) (2010) 1849–1862.
[14] D.P. Mondal, S. Das, N. Jha, Dry sliding wear behaviour of aluminum syntactic foam, Mater. Des. 30 (7) (2009) 2563–2568.
[15] V. Manakari, G. Parande, M. Gupta, Effects of hollow fly-ash particles on the properties of magnesium matrix syntactic foams: a review, Mater. Perform. Charact. 5 (1) (2016) 116–131.
[16] J.-C. Lin, Compression and wear behavior of composites filled with various nano-particles, Compos. Part B: Eng. 38 (1) (2007) 79–85.
[17] S. Bahadur, C. Sunkara, Effect of transfer film structure, composition and bonding on the tribological behavior of polyphenylene sulfide filled with nano particles ofTiO2, ZnO, CuO and SiC, Wear 258 (9) (2005) 1411–TiO1421.
[18] B. Wetzel, F. Haupert, K. Friedrich, M.Q. Zhang, M.Z. Rong, Impact and wear resistance of polymer nanocomposites at low filler content, Polym. Eng. Sci. 42 (9) (2002) 1919–1927.
[19] R.V. Kurahatti, A.O. Surendranathan, S. Srivastava, N. Singh, A.V. Ramesh Kumar, B. Suresha, Role of zirconia filler on friction and dry sliding wear behaviour of bismaleimide nanocomposites, Mater. Des. 32 (5) (2011) 2644–2649.
[20] F. Li, K.-A. Hu, J.-L. Li, B.-Y. Zhao, The friction and wear characteristics of nanometer ZnO filled polytetrafluoroethylene, Wear 249 (10–11) (2001) 877–882.
[21] B.R. Bharath Kumar, S.E. Zeltmann, M. Doddamani, N. Gupta, Uzma, S. Gurupadu, R.R.N. Sailaja, Effect of cenosphere surface treatment and blending method on the tensile properties of thermoplastic matrix syntactic foams, J. Appl. Polym. Sci. 133 (2016) 35.
[22] B.R. Bharath Kumar, M. Doddamani, S.E. Zeltmann, N. Gupta, S. Ramakrishna, Data characterizing tensile behavior of cenosphere/HDPE syntactic foam, Data Brief. 6 (2016) 933–941.
[23] S.E. Zeltmann, B.R. Bharath Kumar, M. Doddamani, N. Gupta, Prediction of strain rate sensitivity of high density polyethylene using integral transform of dynamic mechanical analysis data, Polymer 101 (2016) 1–6.
[24] K. Shahapurkar, C.D. Garcia, M. Doddamani, G.C. Mohan Kumar, P. Prabhakar, Compressive behavior of cenosphere/epoxy syntactic foams in arctic conditions, Compos. Part B: Eng. 135 (2018) 253–262.
[25] S. Waddar, P. Jeyaraj, M. Doddamani, Influence of axial compressive loads on buckling and free vibration response of surface-modified fly ash cenosphere/epoxy syntactic foams, J. Compos. Mater. (2018) (p. 0021998317751284).
[26] B.K. Satapathy, A. Das, A. Patnaik, Ductile-to-brittle transition in cenosphere-filled polypropylene composites, J. Mater. Sci. 46 (6) (2011) 1963–1974.
[27] J. Qiao, G. Wu, Tensile properties of fly ash/polyurea composites, J. Mater. Sci. 46 (11) (2011) 3935–3941.
[28] M.V. Deepthi, M. Sharma, R.R.N. Sailaja, P. Anantha, P. Sampathkumaran, S. Seetharamu, Mechanical and thermal characteristics of high density polyethylene–fly ash cenospheres composites, Mater. Des. 31 (4) (2010) 2051–2060.
[29] S. Ren, X. Tao, X. Ma, J. Liu, H. Du, A. Guo, J. Xu, J. Liang, S. Chen, J. Ge, Fabrication of fly ash cenospheres-hollow glass microspheres/borosilicate glass

composites for high temperature application, Ceram. Int. 44 (1) (2018) 1147–1155.
[30] C. Wang, J. Liu, H. Du, A. Guo, Effect of fly ash cenospheres on the microstructure and properties of silica-based composites, Ceram. Int. 38 (5) (2012) 4395–4400.
[31] M.-R. Wang, D.-C. Jia, P.-G. He, Y. Zhou, Microstructural and mechanical characterization of fly ash cenosphere/metakaolin-based geopolymeric composites, Ceram. Int. 37 (5) (2011) 1661–1666.
[32] V. Manakari, G. Parande, M. Doddamani, V.N. Gaitonde, I.G. Siddhalingeshwar, Kishore, V.C. Shunmugasamy, N. Gupta, Dry sliding wear of epoxy/cenosphere syntactic foams, Tribology Int. 92 (2015) 425–438.
[33] A.K. Singh, Siddhartha, Leverage of cenosphere filler size on mechanical and dry sliding wear peculiarity of polyester composites, J. Compos. Mater. 49 (22) (2015) 2789–2802.
[34] S.R. Chauhan, S. Thakur, Effects of particle size, particle loading and sliding distance on the friction and wear properties of cenosphere particulate filled vinylester composites, Mater. Des. 51 (2013) 398–408.
[35] N. Chand, P. Sharma, M. Fahim, Abrasive wear behavior of LDPE filled with silane treated flyash cenospheres, Compos. Interfaces 18 (7) (2011) 575–586.
[36] D. Ray, R. Gnanamoorthy, Friction and wear behavior of vinylester resin matrix composites filled with fly ash particles, J. Reinf. Plast. Compos. 26 (1) (2007) 5–13.
[37] M. Labella, S.E. Zeltmann, V.C. Shunmugasamy, N. Gupta, P.K. Rohatgi, Mechanical and thermal properties of fly ash/vinyl ester syntactic foams, Fuel 121 (2014) 240–249.
[38] M.M. Hossain, K. Shivakumar, Compression fatigue performance of a fire resistant syntactic foam, Compos. Struct. 94 (1) (2011) 290–298.
[39] M. Doddamani, V.C. Kishore, N. Shunmugasamy, Gupta, H.B. Vijayakumar, Compressive and flexural properties of functionally graded fly ash cenosphere–epoxy resin syntactic foams, Polym. Compos. 36 (4) (2015) 685–693.
[40] W. Wang, Q. Li, B. Wang, X.-T. Xu, J.-P. Zhai, Synthesis of fly ash cenosphere/polyaniline and mullite/polyaniline core–shell composites, Mater. Chem. Phys. 135 (2) (2012) 1077–1083.
[41] S. Guhanathan, M.S. Devi, V. Murugesan, Effect of coupling agents on the mechanical properties of fly ash/polyester particulate composites, J. Appl. Polym. Sci. 82 (7) (2001) 1755–1760.
[42] M. Federici, G. Straffelini, S. Gialanella, Pin-on-disc testing of low-metallic friction material sliding against HVOF coated cast iron: modelling of the contact temperature evolution, Tribol. Lett. 65 (4) (2017) 121.
[43] B. Rashid, Z. Leman, M. Jawaid, M. Ghazali, M. Ishak, M. Abdelgnei, Dry sliding wear behavior of untreated and treated sugar palm fiber filled phenolic composites using factorial technique, Wear 380 (2017) 26–35.
[44] P.C. Verma, R. Ciudin, A. Bonfanti, P. Aswath, G. Straffelini, S. Gialanella, Role of the friction layer in the high-temperature pin-on-disc study of a brake material, Wear 346 (2016) 56–65.
[45] B.R. Bharath Kumar, M. Doddamani, S.E. Zeltmann, N. Gupta, Uzma, S. Gurupadu, R.R.N. Sailaja, Effect of particle surface treatment and blending method on flexural properties of injection-molded cenosphere/HDPE syntactic foams, J. Mater. Sci. 51 (8) (2016) 3793–3805.
[46] G. Straffelini, P.C. Verma, I. Metinoz, R. Ciudin, G. Perricone, S. Gialanella, Wear behavior of a low metallic friction material dry sliding against a cast iron disc: role of the heat-treatment of the disc, Wear 348 (2016) 10–16.
[47] G. Straffelini, L. Maines, The relationship between wear of semimetallic friction materials and pearlitic cast iron in dry sliding, Wear 307 (1–2) (2013) 75–80.
[48] C.E. Dunlap III, Disc Brake Rotor Portion, Google Patents, 2016.
[49] J. Bijwe, Composites as friction materials: recent developments in non-asbestos fiber reinforced friction materials—a review, Polym. Compos. 18 (3) (1997) 378–396.
[50] A.E. Anderson, Friction and Wear of Automotive Brakes, ASM International, 1992.
[51] G. Straffelini, M. Pellizzari, A. Molinari, Influence of load and temperature on the dry sliding behaviour of Al-based metal-matrix-composites against friction material, Wear 256 (7–8) (2004) 754–763.
[52] R.N. Rao, S. Das, Effect of sliding distance on the wear and friction behavior of as cast and heat-treated Al–SiCp composites, Mater. Des. 32 (5) (2011) 3051–3058.
[53] C. Kanchanomai, N. Noraphaiphipaksa, Y. Mutoh, Wear characteristic of epoxy resin filled with crushed-silica particles, Compos. Part B: Eng. 42 (6) (2011) 1446–1452.
[54] Siddhartha, K. Gupta, Mechanical and abrasive wear characterization of bidirectional and chopped E-glass fiber reinforced composite materials, Mater. Des. 35 (2012) 467–479.
[55] M.J. Ghazali, W.M. Rainforth, H. Jones, Dry sliding wear behaviour of some wrought, rapidly solidified powder metallurgy aluminium alloys, Wear 259 (1–6) (2005) 490–500.
[56] A. Shalwan, B.F. Yousif, Influence of date palm fibre and graphite filler on mechanical and wear characteristics of epoxy composites, Mater. Des. 59 (2014) 264–273.
[57] B.-B. Jia, T.-S. Li, X.-J. Liu, P.-H. Cong, Tribological behaviors of several polymer–polymer sliding combinations under dry friction and oil-lubricated conditions, Wear 262 (11–12) (2007) 1353–1359.
[58] K. Kato, Wear in relation to friction — a review, Wear 241 (2) (2000) 151–157.
[59] B. Rashid, Z. Leman, M. Jawaid, M.J. Ghazali, M.R. Ishak, M.A. Abdelgnei, Dry sliding wear behavior of untreated and treated sugar palm fiber filled phenolic composites using factorial technique, Wear 380–381 (2017) 26–35.
[60] J.A.K. Gladston, I. Dinaharan, N.M. Sheriff, J.D.R. Selvam, Dry sliding wear behavior of AA6061 aluminum alloy composites reinforced rice husk ash particulates produced using compocasting, J. Asian Ceram. Soc. 5 (2) (2017) 127–135.
[61] N. Jha, A. Badkul, D.P. Mondal, S. Das, M. Singh, Sliding wear behaviour of aluminum syntactic foam: a comparison with Al–10 wt% SiC composites, Tribol. Int. 44 (3) (2011) 220–231.
[62] Sudarshan, M.K. Surappa, Dry sliding wear of fly ash particle reinforced A356 Al composites, Wear 265 (3) (2008) 349–360.
[63] S. Thakur, S.R. Chauhan, Study on mechanical and tribological behavior of cenosphere filled vinylester composites - a Taguchi method, Indian J. Eng. Mater. Sci. 20 (2013) 10.
[64] M. Doddamani, G. Parande, V. Manakari, I. Siddhalingeshwar, V. Gaitonde, N. Gupta, Wear response of walnut-shell-reinforced epoxy composites, Mater. Perform. Charact. 6 (1) (2017) 25.